JTTEE5 2:165-172

The Influence of Powder Agglomeration Methods on Plasma Sprayed Yttria Coatings

P. Diez and R.W. Smith

Among commercially available powders for plasma spraying, precipitation-calcined processed (PCP) powders have not been used due to the presence of agglomerates, which produce coatings with closed pores. This investigation studied the behavior of PCP agglomerates during plasma spraying. Two PCP yttria powders were selected and air plasma sprayed. Splat morphology and coating microstructure were characterized under various conditions of plasma parameters (i.e., plasma jet enthalpy, nozzle design, spraying distance). A model for agglomerate behavior on impact is proposed to explain microstructural variations and to enable the development of spray parameters that yield dense coatings.

1. Introduction

In the manufacture of engineered plasma sprayed ceramic coatings, characteristics of the starting powder are critical. As recently reported,[1] powder characteristics have a significant influence on the final properties of the coating. Commercially available powders are processed by different routes, each yielding specific powder characteristics. The most commonly used ceramic powders in plasma spraying are

- *Fused and crushed:* produced by the crushing of a sintered body
- *Agglomerated:* resulting from the agglomeration of small particulate material with an organic binder (spray dry process)
- *Agglomerated and sintered:* resulting from the spray dry process followed by a densification step

Optimization of plasma process parameters with such powders to yield coatings with acceptable properties is well documented.[2] However, another less common form of ceramic oxide powder derived from the precipitation-calcination process (PCP powder) is less well understood. PCP powder production, for any yttria powder, consists of the following steps:

- Dissolution of an organic compound in yttrium-bearing solution (for example urea in yttrium nitrate)[3]
- Precipitation of yttrium-bearing organic compound, called the precursor (for example yttrium hydroxycarbonate, see Ref 3)
- Precursor calcination in air, which transforms the yttrium compound into yttrium oxide powder

Keywords: agglomeration, microstructure, morphology, optimization, powder processing, splat structure, yttria powders

P. Diez, Comurhex-Pierrelatte, BP 29, 26701 Pierrelatte Cedex; and **R.W. Smith,** Center for Plasma Processing of Materials, Drexel University, Dept. of Materials Engineering, Philadelphia, Pennsylvania.

PCP powders have seldom been used in plasma processing because this process yields a more dispersed particle size distribution, irregular particle shapes, and a large degree of interparticle agglomeration. Despite the low cost of PCP powders, these drawbacks have limited their use because they cannot be used to plasma spray dense coatings. The purpose of this work was to demonstrate that the plasma spraying process is flexible enough to produce coatings with acceptable density levels (>90%) regardless of the starting powder. PCP yttria (Y_2O_3) powders were selected, and plasma-sprayed coating microstructural variations were studied as a function of process parameters (i.e., nozzle, plasma enthalpy, spraying distance, etc.).

2. Experimental Procedure

Two PCP powders were selected for this study. Each was characterized for mean diameter, size distribution, and particle morphology, using scanning electron microscopy (SEM) observation and laser-scattering measurements (Microtrac™). Size distribution results obtained with each measurement technique were compared. The relevance of this comparison was reported in a previous work,[4] in that a powder composed of weak agglomerates exhibited an apparent mean particle diameter measured by Microtrac™ much lower than the one measured by SEM observation. This experimental evidence resulted from the breakup of agglomerates caused by the turbulent aqueous media used for particle dispersion in the Microtrac™ measurement technique. A significant difference between the two measurement techniques was therefore considered as an indication of the mechanical strength of the agglomerates.

The next step consisted of an investigation of splat and coating microstructure with each powder. Spraying was performed at atmospheric pressure in air. The powder carrier gas flow rate was selected to achieve optimum coating substrate targeting and a uniform spraying pattern.

The following plasma processing parameters were varied (Table 1):

- *Nozzle design:* Two types of nozzles were used. One was equipped with downstream injection powder ports (EPI™ 120), whereas the other (EPI™ 093) had upstream injec-

Table 1 Plasma processing parameters used to spray PCP powders in current study

Sample No.	EPI (a) nozzle	Particle residence time	Plasma gas composition and flow rates Argon, slm	Hydrogen, slm	Power, kW	Plasma enthalpy, kJ/l	Spraying distance, cm
A1	93	High	75.5	7.5	64	29.9 (medium)	7.5 (short)
A2	120	Low	75.5	7.5	63	29.9 (medium)	7.5 (short)
A3	93	High	117.9	7.5	60	18.2 (low)	8.75 (medium)
A4	93	High	89.62	7.5	60	24.1 (low)	8.75 (medium)
A5	93	High	75.5	7.5	64	29.9 (medium)	8.75 (medium)
A6	120	Low	75.5	7.5	64	29.9 (medium)	8.75 (medium)
A7	120	Low	75.5	11.8	72	33.2 (high)	8.75 (medium)
A8	93	High	75.5	11.8	72	33.2 (high)	8.75 (medium)
A9	120	Low	89.6	7.5	54	21.4 (low)	10 (long)
A10.....	120	Low	82.5	8.4	60	26 (medium)	10 (long)
A11.....	93	High	75.5	7.5	75	34.4 (high)	10 (long)
A12.....	120	Low	75.5	10.5	72	33.1 (high)	10 (long)
B1.....	93	High	141.5	7.5	57	14.3 (low)	8.75 (medium)
B2.....	93	High	117.7	7.5	60	18.8 (low)	8.75 (medium)
B3.....	93	High	75.5	7.5	64	29.9 (medium)	8.75 (medium)
B4.....	93	High	70.5	9.8	68	33.8 (high)	7.5 (short)
B5.....	93	High	70.5	9.8	68	33.8 (high)	10 (long)

(a) Electro-Plasma Inc., Irvine, CA.

tion powder ports. This latter nozzle was designed to provide a longer particle residence time in the hotter part of the plasma jet.

- *Plasma jet enthalpy:* Defined as the following ratio:[5]

  Enthalpy (J/l) = power (W) × thermal efficiency (%)/arc gas flow rate (l/s)

  Plasma jet enthalpy was varied by using argon/hydrogen plasma gas mixtures of different composition ratios and by varying the arc current, yielding low (<22 kJ/l) to medium (22 to 32 kJ/l) and high (>32 kJ/l) enthalpy levels. Thermal efficiency was assumed constant (65%) for the set of parameters tested.

- *Spraying distance:* See Table 1.

The splat and coating characterization steps consisted of evaluation of splat degree of melting by SEM observation of splats on glass slides, optical microscope observation of coating density on as-polished coatings, and optical microscope and SEM observation of coating microstructure.

As-polished coating cross sections were etched by immersion in phosphoric acid to reveal boundaries between splats or particles. Fully melted particles spread to form disc-like splats, which appeared as lamellae in cross section. Unmelted or resolidified particles spread to a lesser extent, because they have a higher apparent viscosity, and remained as conical bulky splats or spherical particles in coating cross sections. These observations enabled the degree of particle melting for specific plasma conditions to be assessed.

3. Results

3.1 *Powder Characterization*

Both powders were produced by similar processes and differed only in size distribution. The mean diameter (d_m) of powder A was 51 μm, whereas powder B had a mean diameter of 34 μm. In addition, the particle size distribution was broader for powder A (10 to 100 μm) than for powder B (10 to 60 μm). SEM powder morphology characterization (Fig. 1 and 2) showed that both powders were agglomerates of cubic crystallites of about 5 to 10 μm size for powder B and 10 to 20 μm for powder A. These primary crystallites were dense and often connected to form agglomerates as large as 100 μm. The largest agglomerates were composed of sufficient primary crystallites to form a closed structure with some degree of inner porosity. Both powders yielded laser-scattering size measurements consistent with both the SEM observation and the results reported by the powder producer. The agglomerates of powders A and B were considered mechanically stable.

3.2 *Splat Characterization*

Microscopic observation of splats collected on glass slides provided information on powder behavior in the plasma jet. Splat diameters were found to be the same order of magnitude as the initial powder diameter. Such results were compared to observations made in a previous work[4] with a powder composed of weak agglomerates. In this case, in-flight agglomerate breakdown created splat diameters one order of magnitude lower than the initial powder diameter. In the present investigation, powders A and B exhibited the opposite behavior. Hence, it was concluded that these agglomerates were mechanically stable in the plasma jet.

Splats were bulky in shape (as shown in Fig. 3a). Among bulky, partially solid splats, resolidified particles of various sizes, often with a hollow core, and partially melted particles were observed (Fig. 3a). The degree of melting for each particle was found to increase with increased plasma enthalpy and for the nozzle design that induced a higher particle residence time in the jet core (i.e., EPI™ 093). The degree of particle melting was higher for powder B (smaller crystallites and agglomerate sizes) than for powder A (see powder B splats in Fig. 3b).

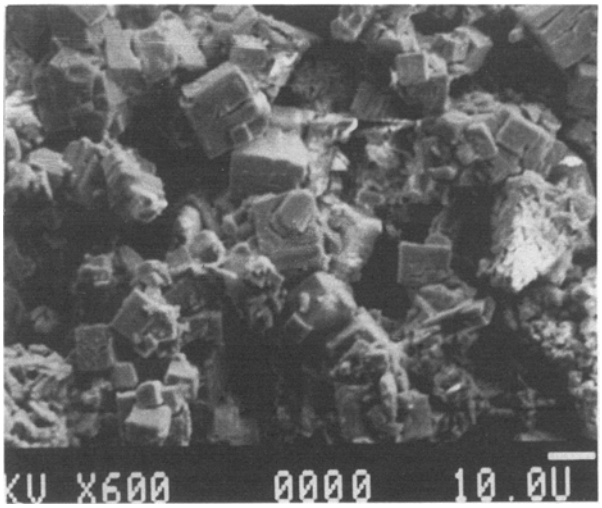

Fig. 1 SEM topography of PCP powder showing agglomerate of cubic crystallites.

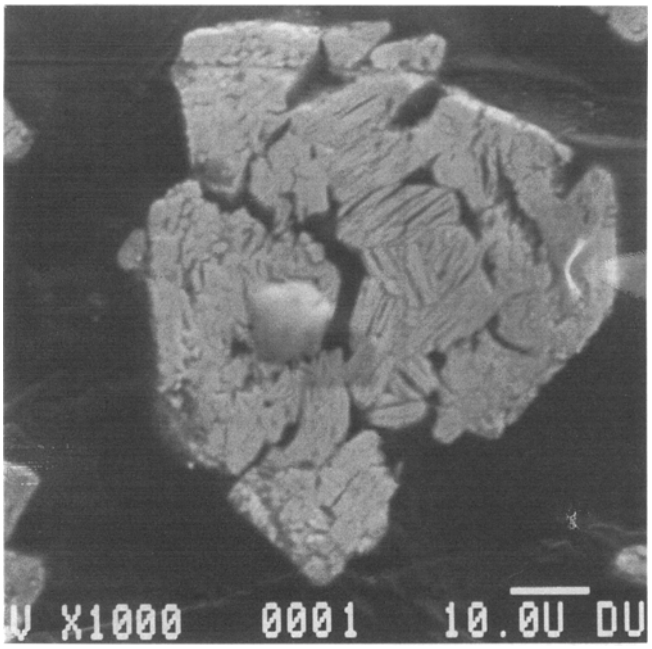

Fig. 2 PCP agglomerate SEM cross section.

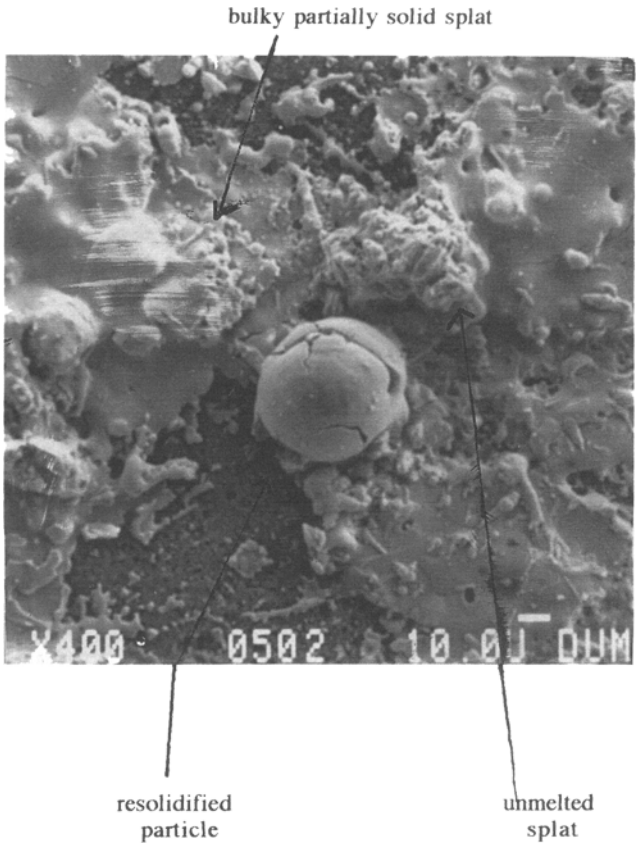

Fig. 3(a) Typical topography of plasma deposited yttria surfaces showing splat structures of PCP powder A (d_m = 51 μm).

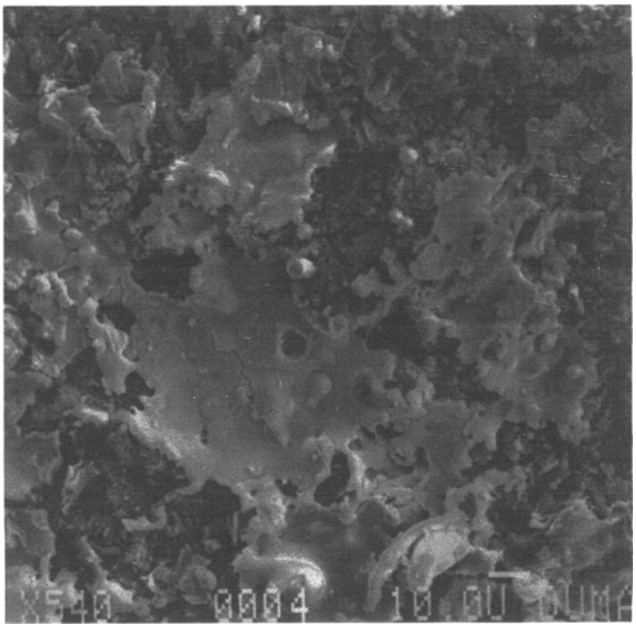

Fig. 3(b) Typical topography of plasma deposited yttria surfaces showing splat structures of PCP powder B (d_m = 34 μm).

3.3 *Coating Density and Microstructure*

3.3.1 *General Aspect*

The degree of lamellar structure content in the as-deposited etched coating was found to increase with increased plasma enthalpy at constant spraying distance and for nozzle designs (EPI™ 093) that induced a higher particle residence time in the plasma jet. Coatings sprayed with the EPI™ 093 nozzle and high plasma enthalpy conditions exhibited a lamellar structure (Fig. 4a) with small columnar grains (1 to 5 μm), whereas coatings sprayed with the EPI™ 120 nozzle, regardless of the plasma enthalpy conditions; and with the EPI™ 093 nozzle, at

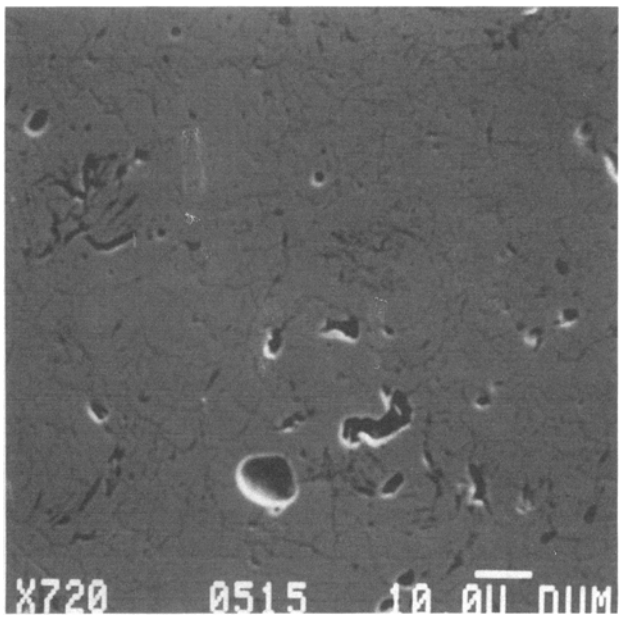

Fig. 4(a) Typical as-etched microstructure of PCP yttria coatings sprayed with EPI™ 093 nozzle and high plasma jet enthalpy (condition A8 in Table 1).

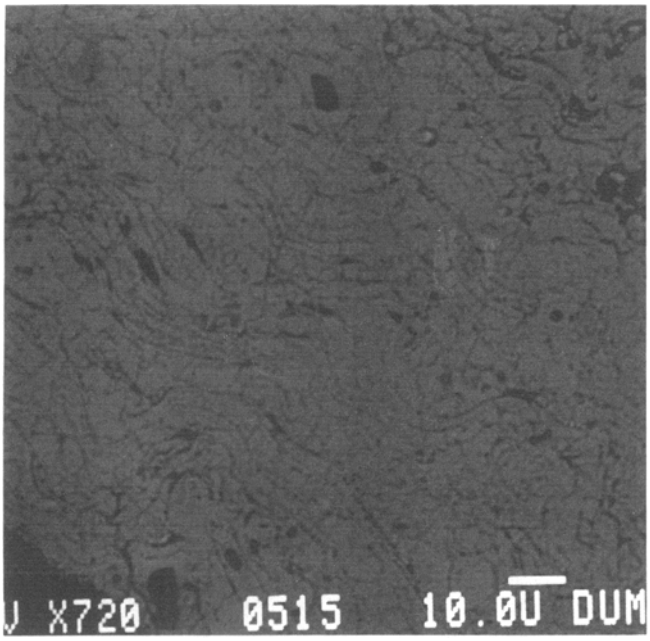

Fig. 4(b) Typical as-etched microstructure of PCP yttria coatings sprayed with EPI™ 120 nozzle and medium to high plasma jet enthalpy (conditions A6 or A7 in Table 1).

lower plasma enthalpy conditions, resulted in a larger grain (5 to 10 μm) equiaxed microstructure in which a lamellar orientation was difficult to distinguish (Fig. 4b). This structure retained much of the agglomerated character of the initial powder.

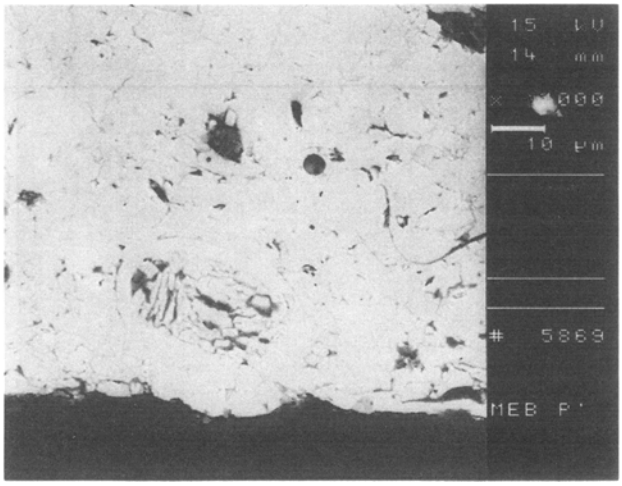

Fig. 5 Typical closed pore S1 structure in as-sprayed etched microstructure of PCP yttria powder A (d_m = 51 μm) coatings sprayed with EPI™ 120 nozzle and medium plasma jet enthalpy (condition A6 in Table 1).

3.3.2 *Closed Porosity*

Closed porosity resulting from the included hollow spheres was an observed microstructural feature found in both powder A (d_m = 51 μm) and B (d_m = 34 μm) deposits. In the case of powder A, the aspect of these entrapped hollow spheres varied as a function of plasma jet enthalpy and nozzle design. With the EPI™ 120 nozzle, regardless of the plasma jet enthalpy conditions, closed pores were formed at the center of a shell composed of crystallites similar to the starting powder A and different from the rest of the melted coating microstructure (closed pore structure S1 shown in Fig. 5a). With the EPI™ 93 nozzle and high plasma jet enthalpy, closed pores were surrounded by shells with layers that had been melted and resolidified, before being trapped in the coating (closed pore structure S2 shown in Fig. 6). Powder B exhibited only structure S2 closed pores in the range of spraying parameters investigated. Finally, for both powders A and B, entrapped hollow sphere concentration increased with increased spraying distance (Fig. 7).

3.3.3 *Effect on Coating Density*

Maximum coating density was reached when the entire coating microstructure consisted of lamellar, well-melted splats, and when closed, entrapped porosity was minimum. This occurred when spraying with the EPI™ 93 nozzle, high plasma jet enthalpy, and short spraying distance (75 mm). In such conditions, coating density was higher for powder B (d_m = 34 μm) than for powder A (d_m = 51 μm). Visual observations of specimens metallography prepared in an identical fashion are shown in Fig. 8.

4. Discussion

Powder A and B agglomerate stability was the dominant factor determining coating microstructure. A model for agglomerate behavior in the plasma jet is proposed in Fig. 9 and 10 and discussed below. The material travel distance inside the plasma

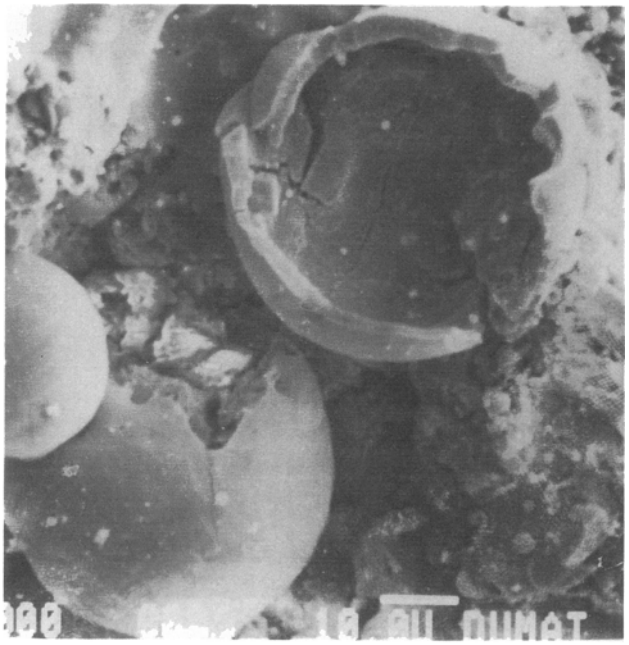

(a)

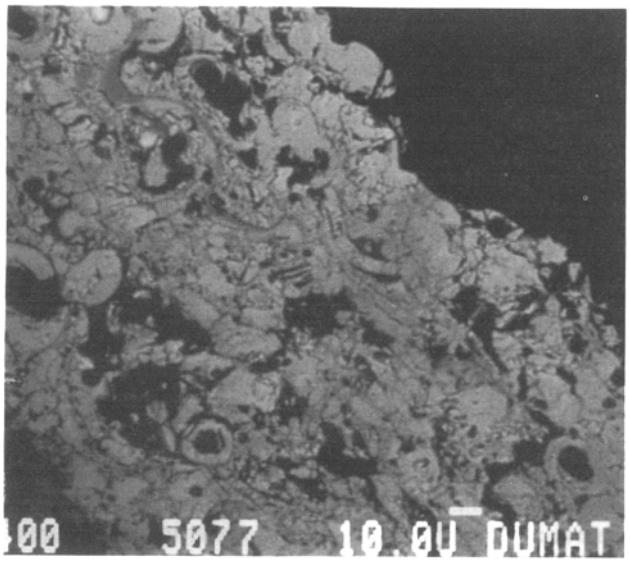

(b)

Fig. 6 Typical aspect of hollow sphere yielding closed pore S2 structure in microstructure of PCP yttria powder B (d_m = 34 μm) coatings sprayed with EPI™ 93 nozzle at high plasma jet enthalpy and long spraying distance (condition B5 in Table 1). (a) SEM aspect of hollow sphere with melted and resolidified shell (S2 structure). (b) Entrapped hollow spheres (S2 structure) in as-sprayed etched microstructure.

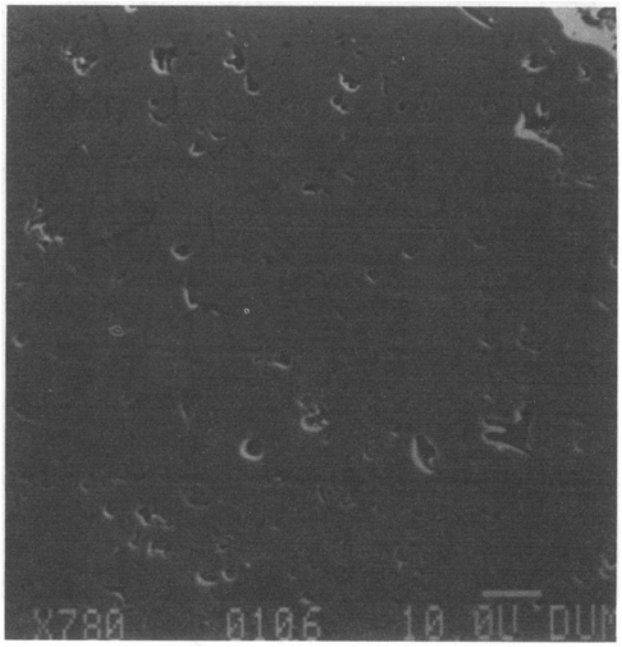

(a)

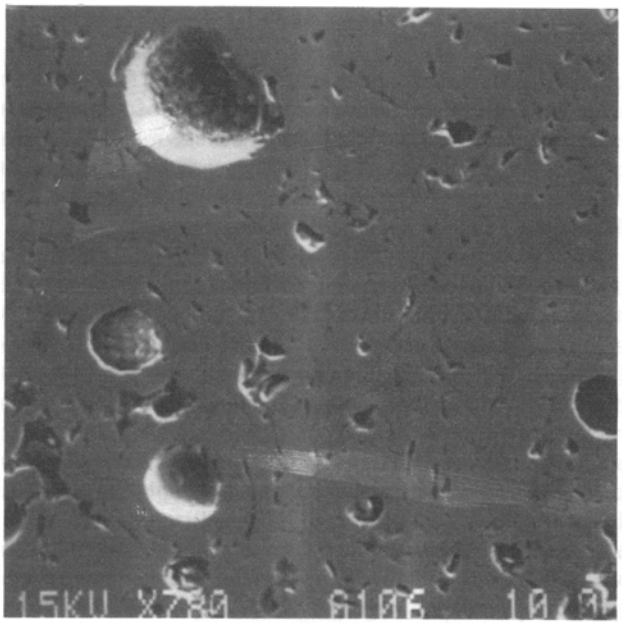

Fig. 7 Effect of spraying distance on concentration of hollow spheres (closed pore S2 structure) in as-sprayed etched microstructures of PCP yttria powder B (d_m = 34 μm). (a) Condition B4 (short spraying distance). (b) Condition B5 (large spraying distance).

jet from its injection to its impact on the substrate was divided into (1) a melting zone, where the material heated up, melted, and eventually superheated; (2) a cooling zone, between the jet tip and the substrate, where the material leaving the melting zone at a higher temperature than the surroundings started to cool, and eventually to solidify; and (3) an impact zone, where the particles hit and deformed on the substrate.

In the proposed model, changes in the agglomerate structure took place in the melting zone. Upon entering the plasma jet, ag-

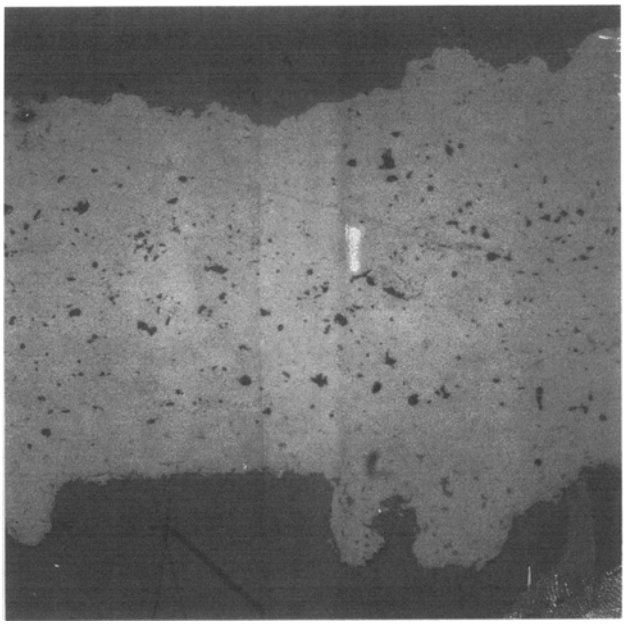

Fig. 8(a) Maximum plasma-sprayed coating density obtained with PCP yttria powder A (d_m = 51 μm) corresponding to condition A8 in Table 1 (high plasma enthalpy, EPI™ 93 nozzle, and short spraying distance of 75 mm).

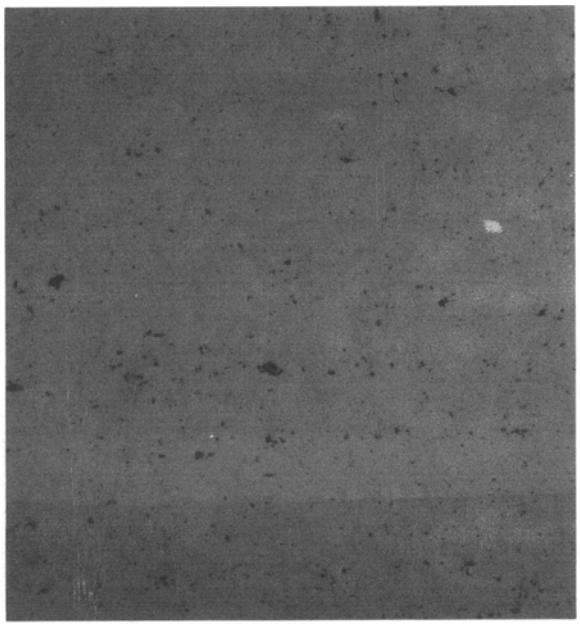

Fig. 8(b) Maximum plasma-sprayed coating density obtained with PCP yttria powder B (d_m = 34 μm) corresponding to condition B4 in Table 1 (high plasma enthalpy, EPI™ 93 nozzle, and short spraying distance of 75 mm).

glomerates started to melt. A continuous melted film formed on their surface, entrapping gas in the agglomerate free space as inner porosity. Due to the low thermal diffusivity of yttria particles, melting of the entire agglomerates was not immediate, but rather a melting front propagated into the agglomerate bulk (see Ref 6).

Hence, depending on spraying conditions, agglomerates could leave the melting zone in different configurations. When spraying with low plasma enthalpy conditions and a nozzle design inducing a short particle residence time in the plasma jet (such as EPI™ 120), agglomerates remained only partially molten and left the melting zone with an outer liquid film, an unmelted solid core, and entrapped inner porosity. When spraying with high plasma enthalpy conditions and a nozzle design inducing a long particle residence time in the plasma jet (EPI™ 093), agglomerates had time to fully melt and left the melting zone as liquid shells with a central inner pore containing gas, which had been already entrapped in the agglomerates upon entering the plasma jet. Large agglomerates (powder A) were more likely to leave the melting zone partially molten. Small agglomerates (powder B), on the other hand, left the melting zone fully molten. Increasing plasma jet enthalpy or switching to a nozzle design inducing a longer particle residence time favored complete melting of larger agglomerates.

Once leaving the hot jet, agglomerates were then submitted to in-flight convective cooling by the cool gas in the cooling zone. The time available for convective cooling to occur increased with spraying distance. Also, because the thermal conductivity of yttria is low, the temperature drop was higher at their surface than in their center. When the surface temperature had dropped to the melting point, solidification began, and a solidification front started to propagate into the agglomerate center.

According to the previous considerations, agglomerates were found to impact the substrate under different melting conditions. They could be partially or completely molten, partially or completely resolidified, and a combination thereof, depending on the spraying conditions. Most agglomerates still contained entrapped porosity. Each agglomerate configuration behaved differently upon impact on the substrate, as illustrated in Fig. 9 and 10. Their behavior determined the resulting coating microstructure and is discussed below.

Agglomerates that arrived fully liquid on the substrate deformed upon impact, spread, and released their entrapped gas (case 1 in Fig. 9). In such cases, the resulting microstructure did not have any initial agglomerate structure, and a large degree of lamellar orientation was observed. Contact between successive splats was good, so that intersplat porosity was low. A typical example of this case could be observed when spraying with nozzle designs inducing a long particle residence time in the jet, at high plasma jet enthalpy conditions, and short spraying distances (Fig. 3a). The splats solidified in a directional fashion and lead to columnar grains oriented in the direction of heat flow.

Agglomerates that had been fully melted and started to resolidify in the cooling zone arrived on the substrate with an outside resolidified shell and a remaining liquid core around its inner pore. Depending on the shell thickness, several cases were possible (cases 2, 3, and 4).

Thin resolidified shells broke up on impact, yielding splats, with pieces of resolidified shell dispersed among the remaining liquid (case 2 in Fig. 9). Such agglomerates were considered re-

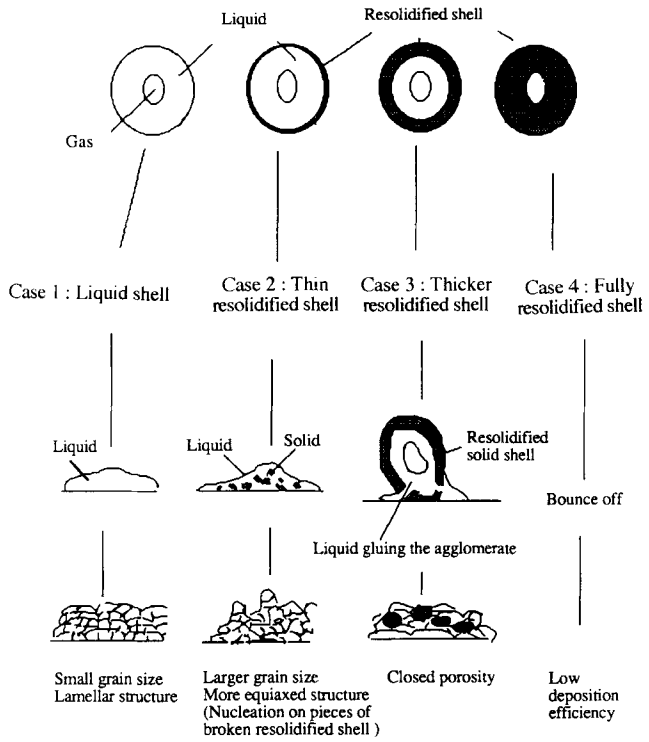

Fig. 9 Suggested agglomerate deformation models originating from fully melted agglomerates.

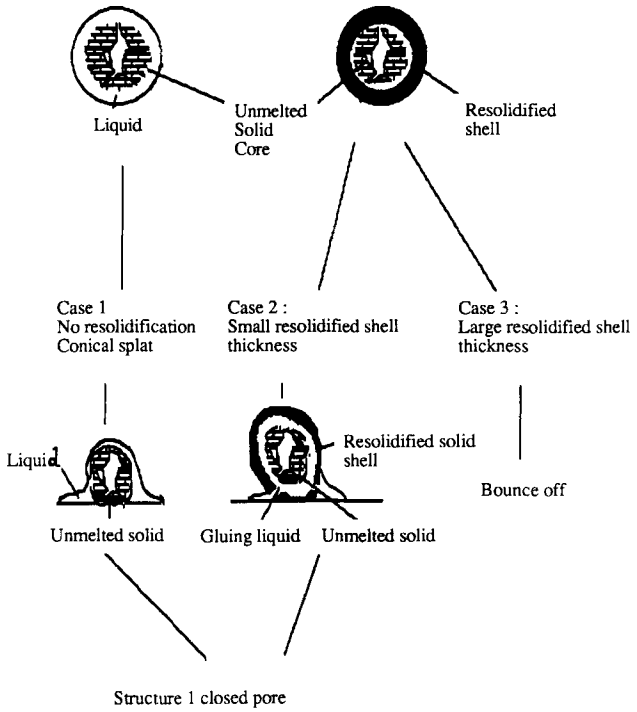

Fig. 10 Suggested agglomerate deformation models originating from incompletely melted agglomerates.

sponsible for the formation of an equiaxed structure observed when spraying with the EPI™ 120 nozzle at medium to high plasma enthalpy conditions (Fig. 3b), as explained by the following. Partially resolidified agglomerates had an apparent viscosity that was higher than fully liquid particles, because of their higher solid fraction. Hence, their degree of spreading was low, and bulky conical splats were expected to result from their impact, yielding coating microstructures with weak lamellar orientation (Fig. 3b). In addition, as a result of the resolidified shell breakdown, small solid particles were dispersed in the liquid and could act as nuclei during splat solidification. This yielded a more randomly oriented equiaxed microstructure, as observed in Fig. 3(b).

Thicker solid shell particles did not fully break on impact, but fractured. If they were not fully resolidified before impact (case 3 in Fig. 9), then the liquid could be released through cracks in the shell. This liquid spread onto the substrate around the impact point and adhered the solid shells to the substrate. Such a mechanism produced closed pores with a fully recrystallized shell in the coating microstructure. This type of closed porosity was commonly observed when spraying with high plasma jet enthalpy, the EPI™ 093 nozzle, and longer spraying distances for powder A and B and has been identified as S2-type porosity (as defined in Fig. 6a and b).

Case 4 in Fig. 10 is an extension of case 2, in which the resolidified shell was so thick that there was not enough liquid inside the particle to adhere the shell to the substrate. Such agglomerates could stick on the substrate by entrapment by another liquid splat. In most cases, these bounced off, especially at long spraying distances, for which low deposition efficiencies were observed.

Agglomerates that were not fully molten in the melting zone arrived on the substrate with a solid inner core. If their liquid shell was thick enough, it deformed readily on impact, adhering the solid core to the substrate (case 1 in Fig. 10). In cross sections, this mechanism corresponded to the closed pore structure S1 (defined in Fig. 5) with an outer recrystallized structure and an inner core composed of unmelted original powder particles and closed pores between them. This structure was typical of powder A when spraying with medium plasma jet enthalpy and medium spraying distance conditions.

For incompletely melted agglomerates, after the melting zone, that were partially resolidified in the cooling zone, the deformation mode on impact depended on the solid shell thickness and on the amount of remaining liquid (cases 2 and 3 in Fig. 10). If they adhered to the substrate, then such agglomerates resulted in closed pores of type S1.

5. Conclusions

This investigation confirmed that yttria powders derived from the precipitation-calcination process were composed of cubic crystallite agglomerates, which were mechanically stable enough to behave as single particles during the spraying proc-

ess. Some agglomerates were made of sufficient primary particles to form a closed structure with some degree of inner porosity. A model of agglomerate behavior in the plasma jet was proposed to explain the observed coating microstructure.

Smaller powder B agglomerates (d_m = 34 μm) were easily melted even when spraying with low plasma enthalpy conditions, but because of their size quickly resolidified. Hence, a short spraying distance (<7 cm) was required to achieve high densities (>90%) and avoid partial inflight resolidification, which caused formation of closed pores. At long spraying distances (>10 cm), agglomerates completely resolidified, and most of them bounced off, yielding low deposition efficiencies.

Large powder A agglomerates (d_m = 51 μm) were often incompletely melted even when spraying with a nozzle providing a long particle residence time in the plasma jet and at high plasma jet enthalpy. These resulted in coating microstructures with closed pores of S1 structure, exhibiting remnants of initial powder particles. When complete resolidification occurred, they deformed, as shown in case 3 in Fig. 10, and usually bounced off. This resulted in the low deposition efficiencies observed for large spraying distance conditions.

This detailed investigation provided a better understanding of agglomerate behavior in the plasma jet and enabled high coating densities. PCP powders, usually of a lower cost, are acceptable for plasma spraying applications despite the presence of agglomerates.

Acknowledgments

The authors would like to thank Péchiney and Uranium Péchiney Corporation for providing support and funding for this investigation.

References

1. E. Kubel, Powders Dictate Thermal Spray Coating Properties, *Adv. Mater. Proc.*, Vol 138 (No. 6), 1990, p 24-32
2. M. Vardelle, A. Vardelle, A. Denoirjean, and P. Fauchais, "Heat Treatment of Zirconia Powders with Different Morphologies under Thermal Spray Conditions," *MRS Spring Meeting 1990 Proc.*, Vol 190, 1990, p 55
3. M. Ciftcioglu, M. Akinc, and L. Burkhart, Effect of Agglomerate Strength on Sintered Density for Yttria Powders Containing Agglomerates of Monosize Spheres, *J. Am. Ceram. Soc.*, Vol 70 (No. 11), 1987, C329-C334
4. P. Diez, "Microstructure and Interface Bonding Studies in Plasma Sprayed Yttria Coatings on Graphite," MS thesis, Drexel University, 1991
5. H.S. Ingham and A.J. Fabel, Comparison of Plasma Spray Gases, *Weld. J.*, Vol 54, 1975, p 101-105
6. E. Bourdin, P. Fauchais, and M. Boulos, Transient Heat Conduction under Plasma Conditions, *Int. J. Heat Mass Transfer*, Vol 26 (No. 4), 1983, p 567-582